Molecular Therapy
Letter to the Editor

Limited astrocyte-to-neuron conversion in the mouse brain using NeuroD1 overexpression

The central nervous system (CNS) is largely unable to generate new neurons to compensate for the loss of neurons caused by disease or injury. One potentially promising approach to replace CNS neurons is to convert resident astrocytes into neurons *in situ* by gene therapy. Conversion of astrocytes to neurons *in vitro* by overexpression of the transcription factor *Pax6* was first reported nearly 20 years ago.[1] Since then, multiple groups have reported astrocyte-to-neuron conversion *in vitro* and *in vivo* following various genetic manipulations.[2–11] Recently, overexpression of NeuroD1[12–17] and knockdown of the RNA splicing factor *Ptbp1*[18,19] were assessed for their ability to convert astrocytes to neurons *in vivo* in multiple CNS areas, with therapeutic effects in mouse models of disease, ischemia, and injury. However, key findings from this work were not readily reproduced,[20] prompting responses from the original authors[21,22] and generating controversy around astrocyte-to-neuron conversion. Here we report limited, brain-area-specific astrocyte-to-neuron conversion in mice and compare our findings with recent reports.

We initially set out to test astrocyte-to-neuron conversion across the mouse CNS using systemic delivery of the blood-brain-barrier-penetrating AAV-PHP.eB capsid[23] and a shortened human *GFAP* promoter (hGFAP)[24] to restrict expression to astrocytes. We achieved improved broad expression in astrocytes with self-complementary AAV genomes[25] (Figures 1A–1C; Figure S1B) and confirmed that miR-124 targeting sites (miR-124-TSs)[26] in the 3′ untranslated region (UTR) helped restrict expression to astrocytes (Figures S1A and S1B). However, the expression level was generally low, and we noted trace levels of off-target expression in neurons (Figures 1C and S1B) as well as scattered expression in the liver (data not shown). These results underscore the difficulty of targeting astrocytes specifically by systemic AAV injection.

We instead decided to permanently label astrocytes with tdTomato (tdTom) in *Aldh1l1*^{CreERT2}; *Rosa26*$^{LSL\text{-}tdTom}$ mice[27] and deliver AAV1 vectors expressing conversion factors directly into the brain parenchyma. Tamoxifen administration in these mice led to tdTom expression in the vast majority of astrocytes, with only rare expression in neurons (data not shown). To test NeuroD1-mediated conversion, we designed expression cassettes with hGFAP promoters driving NeuroD1.P2A.EGFP or EGFP alone. Both cassettes included the 3′UTR miR-124-TS. We also designed an artificial microRNA[28] targeting *Ptbp1* (miPtbp1) and confirmed its activity *in vitro* (Figure S1C). We then cloned miPtbp1 or a control microRNA[29] (miControl) into the 3′UTR of a hGFAP-EGFP transgene. Four weeks after tamoxifen administration, we infused AAV1 vectors with each of these four transgenes unilaterally into the striatum, hippocampus, and cerebellum at 1×10^9 vector genomes (vg) per injection site (Figure 1D). We perfused the mice after 4 weeks and collected their brains for histology.

We next performed immunofluorescence for the neuronal marker NeuN to identify fate-mapped tdTom-positive cells that had converted to neuron-like cells. In mice treated with NeuroD1, we observed extensive tdTom/NeuN overlap in the hippocampus and cerebellar cortex but not in the striatum (Figures 1E and 1F). In the hippocampus, viral expression was largely confined to the molecular layers of the dentate gyrus (DG) and cornu ammonis 1 (CA1), and apparent conversion was entirely confined to these regions (Figure S1D). Concerningly, conversion in the cerebellar cortex was localized to regions with a damaged granule cell layer (Figure S1D). In the hippocampus and cerebellar cortex, conversion was always within a few hundred micrometers of the needle track. However, despite the proximity to the needle track, NeuN staining in the far-red channel in converted cells was not due to autofluorescence, which was punctate and faint (data not shown). In addition, the hGFAP promoter remained active in induced NeuN-positive cells, unlike in mature neurons, because we noted continued EGFP expression (Figures 1E and 1F). In contrast to NeuroD1, we observed no evidence of astrocyte-to-neuron conversion in mice treated with the EGFP control virus (Figure S1E), miPtbp1 virus (Figure 1G; Figure S1D), or miControl virus (data not shown).

Although the NeuroD1 results were encouraging, apparent astrocyte-to-neuron conversion occurred in a narrow region close to the injection site. It has been proposed that reactive astrocytes may be more readily converted into neurons than nonreactive astrocytes.[30] Therefore, we decided to test astrocyte-to-neuron conversion in *Tpp1*$^{-/-}$ mice,[31] a model of late infantile neuronal ceroid lipofuscinosis. These mice develop progressive astrogliosis beginning by 9 weeks of age and some neurodegeneration by the end stage at 21 weeks.[32] As expected, we observed elevated levels of the reactive astrocyte marker Gfap by 11 weeks of age that increased by 14 weeks (Figure S1F). We next infused the cerebral cortex, striatum, hippocampus, and cerebellum of 10-week-old *Tpp1*$^{-/-}$ mice with 1×10^9 vg of the same viruses as above (Figure 1H). To identify converted neurons, we performed NeuN immunofluorescence and identified transduced astrocytes by EGFP expression. In NeuroD1-treated *Tpp1*$^{-/-}$ mice, we detected no EGFP/NeuN overlap in the cerebral cortex (Figure 1I). In brain areas tested previously in *Aldh1l1*^{CreERT2}; *Rosa26*$^{LSL\text{-}tdTom}$ mice, results were comparable in *Tpp1*$^{-/-}$ mice; we observed no NeuN/EGFP overlap in the striatum but significant overlap in the molecular layers of the hippocampus and in the cerebellar cortex (Figure 1I). As above, cerebellar regions with apparent conversion were marked by a damaged granule cell layer, and we noted particularly strong Gfap expression in these areas (Figures 1I). We again saw no evidence of astrocyte-to-neuron conversion in *Tpp1*$^{-/-}$ mice injected with EGFP control (Figure S1G) or miPtbp1 viruses (data not shown). Therefore, the astrogliosis in *Tpp1*$^{-/-}$ mice did not enhance astrocyte-to-neuron conversion compared with wild-type mice.

In summary, we observed evidence of NeuroD1-mediated astrocyte-to-neuron conversion in the mouse hippocampus and cerebellar cortex but not in the cerebral cortex

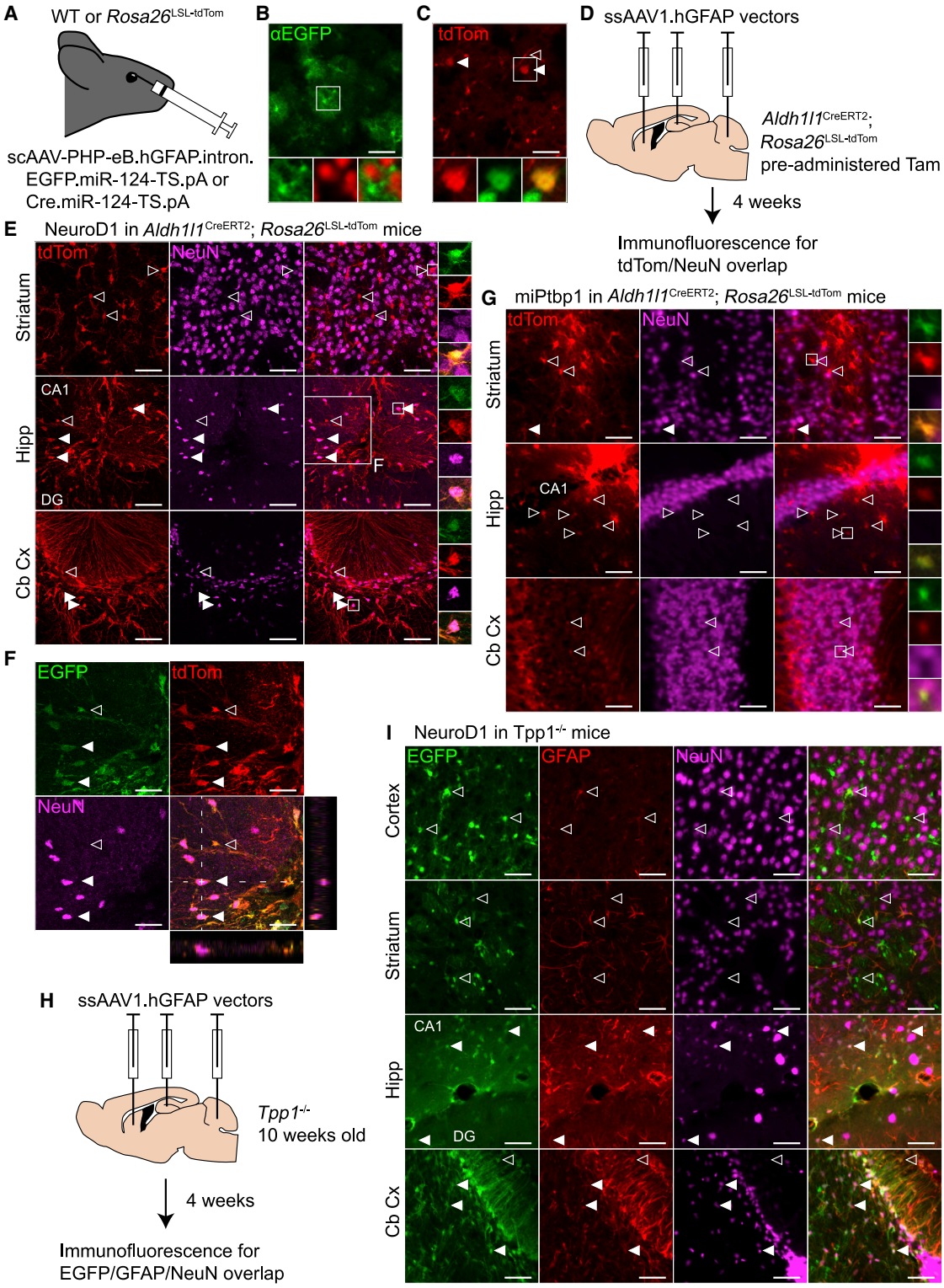

Figure 1. Overexpression of NeuroD1 induces NeuN expression in astrocytes in the mouse hippocampus and cerebellar cortex

(A) Optimized AAVs expressing EGFP (3.16×10^{11} vg) or Cre (1.00×10^{11} vg) from a hGFAP promoter were injected retro-orbitally into wild-type (WT) or *Rosa26*$^{LSL\text{-}tdTom}$ mice, respectively. (B) Widespread but faint EGFP immunofluorescence (green, main and bottom left) did not co-localize with NeuN immunofluorescence (red, bottom center)

(legend continued on next page)

or striatum. Where conversion was observed, it was limited spatially to within a few hundred micrometers of the injection site. This may be due to a localized dose effect or damage and inflammation along the needle track. In addition, converted cells were likely not fully mature neurons by 4 weeks after injection because the hGFAP promoter remained highly active in these cells. We did not follow converted cells for a longer time period because of the limited scope of conversion. In contrast to NeuroD1 overexpression, delivery of an artificial microRNA targeting *Ptbp1* did not lead to astrocyte-to-neuron conversion in any brain area, although we did not quantify *Ptbp1* knockdown *in vivo*. One caveat regarding our results is the small scale of this pilot study. However, the results were consistent across multiple animals in two mouse lines, including *Aldh1l1*^{CreERT2} mice, which enable robust fate mapping of astrocytes. We also note that *Aldh1l1* and *Gfap*, the genes on which our Cre and AAV reporter systems are based, are expressed in neural stem cells in the subgranular zone (SGZ), which normally generate granule cells in the DG granule cell layer. Thus, it is possible that neural stem cells, rather than astrocytes, gave rise to the apparent converted neurons in the hippocampus. This possibility is made less likely by the distance between the SGZ and the converted neurons, the farthest of which were across the hippocampal fissure in CA1, and the relatively short time frame of the experiments.

Published results on astrocyte-to-neuron conversion using NeuroD1 overexpression vary widely.[12–14,16,17,30] In a recent publication, Wang et al.[20] propose that the *Neurod1* DNA sequence upregulates GFAP promoter activity in neurons and that this can lead to spurious reports of astrocyte-to-neuron conversion. When they instead fate mapped astrocytes in *Aldh1l1*^{CreERT2}; *Rosa26*$^{LSL\text{-}tdTom}$ mice, as we did above, they reported no NeuroD1-mediated conversion in the cerebral cortex and striatum. This is consistent with our results showing a lack of conversion in these brain areas but some conversion in the hippocampus and cerebellar cortex. However, Xian et al.[22] do report conversion in the cerebral cortex and striatum in these mice. We cannot rule out the possibility of efficient conversion in the cerebral cortex and striatum with alternative viral vectors, a higher dose, or a longer time period after injection. Similar to NeuroD1-mediated conversion, widely varying efficiencies of astrocyte-to-neuron conversion by *Ptbp1* knockdown have been reported.[18–20,33] The degree of *in vivo* knockdown of *Ptbp1* is difficult to compare between these studies and may be critical to achieve efficient conversion. Overall, we are concerned by how difficult it is to reproduce efficient astrocyte-to-neuron conversion. Additional work is clearly needed to verify the results of *in vivo* conversion experiments and establish the precise conditions that permit conversion.

Although astrocyte-to-neuron conversion may be possible, important questions remain unanswered regarding its therapeutic application. For us, NeuN expression was only induced in astrocytes very close to the injection site. Conversion on this scale is unlikely to have a therapeutic effect in the mouse brain and even less likely in the much larger human brain. Therefore, the route of administration and dose will have to be carefully considered to optimize conversion while minimizing toxicity. Systemic delivery of AAVs may be an option for broader conversion, but this would likely require a high dose of AAVs and lead to unintended expression in the periphery, as noted above for AAV-PHP.eB in mice. If more widespread conversion is achievable, long-term studies using rigorous methods will be needed to determine whether induced NeuN-positive cells develop into mature neurons that can integrate into neural circuits and rescue disease phenotypes. Although these are major challenges, it may be premature to abandon astrocyte-to-neuron conversion without further investigation.

SUPPLEMENTAL INFORMATION

Supplemental information can be found online at https://doi.org/10.1016/j.ymthe.2022.01.028.

ACKNOWLEDGMENTS

We thank Kasey Brida, Laurence Busque, and Mary Doan for AAV vector preparation. The project was (in part) supported by award T32NS007413 from the National Institute of Neurological Disorders and Stroke (NINDS). The content is the sole responsibility of the authors and does not necessarily represent the official views of the NINDS of the National Institutes of Health.

AUTHOR CONTRIBUTIONS

D.L. designed the research, performed experiments, and analyzed data. D.L. and A.M.M. designed the artificial microRNA targeting *Ptbp1*. Y.H.C. and A.M.M. designed the ITR block sequence. B.L.D. designed and supervised the research. D.L. and B.L.D. wrote the manuscript with input from all authors.

in the primary visual cortex after AAV administration in WT mice (n = 2). Scale bar, 50 μm. (C) tdTom fluorescence (red, main and bottom left) and NeuN immunofluorescence (green, bottom center) in primary visual cortex following AAV administration in *Rosa26*$^{LSL\text{-}tdTom}$ mice (n = 2). Solid arrowheads, tdTom- and NeuN-positive neurons; open arrowhead, tdTom-positive endothelial cell. Scale bar, 50 μm. (D) ssAAV1 vectors with conversion factors or controls were infused into the striatum, hippocampus, and cerebellum in *Aldh1l1*^{CreERT2}; *Rosa26*$^{LSL\text{-}tdTom}$ mice at a dose of 1×10^9 vg per site. Mice were perfused after 4 weeks for histology. (E) tdTom and NeuN immunofluorescence following NeuroD1 overexpression in the striatum, the molecular layers of the DG and CA1 in the hippocampus, and the cerebellar cortex (n = 2). All cells marked with arrowheads are tdTom+ and EGFP+. Closed arrowheads represent transduced, fate-mapped astrocytes that express NeuN. Scale bars, 50 μm. (F) Magnification of the hippocampus in (E), showing co-localization of EGFP, dTom, and NeuN, with orthogonal views through a NeuN+ cell. Scale bars, 100 μm. (G) Fluorescence images following miPtbp1 expression with the same channels and brain areas as in (E). Only a low, background level of tdTom/NeuN co-localization was observed (n = 1). Scale bars, 50 μm. (H) 10-week-old *Tpp1*$^{-/-}$ mice were infused with the same viruses as the *Aldh1l1*^{CreERT2}; *Rosa26*$^{LSL\text{-}tdTom}$ mice, with an added infusion in the cerebral cortex above the hippocampus. Mice were perfused after 4 weeks for histology. (I) Immunofluorescence images from *Tpp1*$^{-/-}$ mice (n = 3) treated with NeuroD1. Shown are EGFP (green, left), Gfap immunofluorescence, and NeuN immunofluorescence in the cerebral cortex, striatum, hippocampus, and cerebellar cortex. Scale bars, 50 μm. In all panels, transduced cells that do and do not colocalize with NeuN are labeled with solid and open arrowheads, respectively. Tam, tamoxifen; Hipp, hippocampus; Cb Cx, cerebellar cortex; DG, dentate gyrus. See also Figure S1.

DECLARATION OF INTERESTS

B.L.D. is on the SAB and/or receives sponsored research support for the laboratory from Homology Medicines, Saliogen Therapeutics, Patch Bio, Moment Bio, Panorama Medicines, Resilience, Spirovant Sciences, Novartis Institute for Biomedical Research, Roche, and Sanofi.

David Leib,[1] Yong Hong Chen,[1] Alex Mas Monteys,[1,2] and Beverly L. Davidson[1,2]

[1]Raymond G. Perelman Center for Cellular and Molecular Therapeutics, Children's Hospital of Philadelphia, Philadelphia, PA 19104, USA; [2]Department of Pathology and Laboratory Medicine, University of Pennsylvania Perelman School of Medicine, Philadelphia, PA 19104, USA

https://doi.org/10.1016/j.ymthe.2022.01.028

Correspondence: Beverly L. Davidson, Raymond G. Perelman Center for Cellular and Molecular Therapeutics, Children's Hospital of Philadelphia, Philadelphia, PA 19104, USA.
E-mail: davidsonbl@chop.edu

REFERENCES

1. Heins, N., Malatesta, P., Cecconi, F., Nakafuku, M., Tucker, K.L., Hack, M.A., Chapouton, P., Barde, Y.A., and Götz, M. (2002). Glial cells generate neurons: the role of the transcription factor Pax6. Nat. Neurosci. *5*, 308–315. https://doi.org/10.1038/nn828.

2. Buffo, A., Vosko, M.R., Ertürk, D., Hamann, G.F., Jucker, M., Rowitch, D., and Götz, M. (2005). Expression pattern of the transcription factor Olig2 in response to brain injuries: implications for neuronal repair. Proc. Natl. Acad. Sci. U S A *102*, 18183–18188. https://doi.org/10.1073/pnas.0506535102.

3. Berninger, B., Costa, M.R., Koch, U., Schroeder, T., Sutor, B., Grothe, B., and Götz, M. (2007). Functional properties of neurons derived from in vitro reprogrammed postnatal astroglia. J. Neurosci. *27*, 8654–8664. https://doi.org/10.1523/JNEUROSCI.1615-07.2007.

4. Heinrich, C., Blum, R., Gascón, S., Masserdotti, G., Tripathi, P., Sánchez, R., Tiedt, S., Schroeder, T., Götz, M., and Berninger, B. (2010). Directing astroglia from the cerebral cortex into subtype specific functional neurons. PLoS Biol. *8*, e1000373. https://doi.org/10.1371/journal.pbio.1000373.

5. Grande, A., Sumiyoshi, K., López-Juárez, A., Howard, J., Sakthivel, B., Aronow, B., Campbell, K., and Nakafuku, M. (2013). Environmental impact on direct neuronal reprogramming in vivo in the adult brain. Nat. Commun. *4*, 2373. https://doi.org/10.1038/ncomms3373.

6. Niu, W., Zang, T., Zou, Y., Fang, S., Smith, D.K., Bachoo, R., and Zhang, C.L. (2013). In vivo reprogramming of astrocytes to neuroblasts in the adult brain. Nat. Cell Biol. *15*, 1164–1175. https://doi.org/10.1038/ncb2843.

7. Torper, O., Pfisterer, U., Wolf, D.A., Pereira, M., Lau, S., Jakobsson, J., Björklund, A., Grealish, S., and Parmar, M. (2013). Generation of induced neurons via direct conversion in vivo. Proc. Natl. Acad. Sci. U S A *110*, 7038–7043. https://doi.org/10.1073/pnas.1303829110.

8. Liu, Y., Miao, Q., Yuan, J., Han, S., Zhang, P., Li, S., Rao, Z., Zhao, W., Ye, Q., Geng, J., Zhang, X., and Cheng, L. (2015). Ascl1 converts dorsal midbrain astrocytes into functional neurons in vivo. J. Neurosci. *35*, 9336–9355. https://doi.org/10.1523/JNEUROSCI.3975-14.2015.

9. Aravantinou-Fatorou, K., Ortega, F., Chroni-Tzartou, D., Antoniou, N., Poulopoulou, C., Politis, P.K., Berninger, B., Matsas, R., and Thomaidou, D. (2015). CEND1 and NEUROGENIN2 reprogram mouse astrocytes and embryonic fibroblasts to induced neural precursors and differentiated neurons. Stem Cell Rep. *5*, 405–418. https://doi.org/10.1016/j.stemcr.2015.07.012.

10. Berninger, B., and Jessberger, S. (2016). Engineering of adult neurogenesis and Gliogenesis. Cold Spring Harb. Perspect. Biol. *8*. https://doi.org/10.1101/cshperspect.a018861.

11. Lei, W., Li, W., Ge, L., and Chen, G. (2019). Non-engineered and engineered adult neurogenesis in mammalian brains. Front. Neurosci. *13*, 131. https://doi.org/10.3389/fnins.2019.00131.

12. Guo, Z., Zhang, L., Wu, Z., Chen, Y., Wang, F., and Chen, G. (2014). In vivo direct reprogramming of reactive glial cells into functional neurons after brain injury and in an Alzheimer's disease model. Cell Stem Cell *14*, 188–202. https://doi.org/10.1016/j.stem.2013.12.001.

13. Chen, Y.C., Ma, N.X., Pei, Z.F., Wu, Z., Do-Monte, F.H., Keefe, S., Yellin, E., Chen, M.S., Yin, J.C., Lee, G., et al. (2020). A NeuroD1 AAV-based gene therapy for functional brain repair after ischemic injury through in vivo astrocyte-to-neuron conversion. Mol. Ther. *28*, 217–234. https://doi.org/10.1016/j.ymthe.2019.09.003.

14. Wu, Z., Parry, M., Hou, X.Y., Liu, M.H., Wang, H., Cain, R., Pei, Z.F., Chen, Y.C., Guo, Z.Y., et al. (2020). Gene therapy conversion of striatal astrocytes into GABAergic neurons in mouse models of Huntington's disease. Nat. Commun. *11*, 1105. https://doi.org/10.1038/s41467-020-14855-3.

15. Ge, L.J., Yang, F.H., Li, W., Wang, T., Lin, Y., Feng, J., Chen, N.H., Jiang, M., Wang, J.H., Hu, X.T., et al. (2020). In vivo neuroregeneration to treat ischemic Stroke through NeuroD1 AAV-based gene therapy in adult non-human primates. Front. Cell Dev. Biol. *8*, 590008. https://doi.org/10.3389/fcell.2020.590008.

16. Puls, B., Ding, Y., Zhang, F., Pan, M., Lei, Z., Pei, Z., Jiang, M., Bai, Y., Forsyth, C., Metzger, M., et al. (2020). Regeneration of functional neurons after spinal cord injury via in situ NeuroD1-mediated astrocyte-to-neuron conversion. Front. Cell Dev. Biol. *8*, 591883. https://doi.org/10.3389/fcell.2020.591883.

17. Tang, Y., Wu, Q., Gao, M., Ryu, E., Pei, Z., Kissinger, S.T., Chen, Y., Rao, A.K., Xiang, Z., Wang, T., et al. (2021). Restoration of visual function and cortical connectivity after ischemic injury through NeuroD1-mediated gene therapy. Front. Cell Dev. Biol. *9*, 720078. https://doi.org/10.3389/fcell.2021.720078.

18. Qian, H., Kang, X., Hu, J., Zhang, D., Liang, Z., Meng, F., Zhang, X., Xue, Y., Maimon, R., Dowdy, S.F., et al. (2020). Reversing a model of Parkinson's disease with in situ converted nigral neurons. Nature *582*, 550–556. https://doi.org/10.1038/s41586-020-2388-4.

19. Zhou, H., Su, J., Hu, X., Zhou, C., Li, H., Chen, Z., Xiao, Q., Wang, B., Wu, W., Sun, Y., et al. (2020). Glia-to-Neuron conversion by CRISPR-CasRx alleviates symptoms of neurological disease in mice. Cell *181*, 590–603.e16. https://doi.org/10.1016/j.cell.2020.03.024.

20. Wang, L.L., Serrano, C., Zhong, X., Ma, S., Zou, Y., and Zhang, C.L. (2021). Revisiting astrocyte to neuron conversion with lineage tracing in vivo. Cell *184*, 5465–5481.e16. https://doi.org/10.1016/j.cell.2021.09.005.

21. Chen, G. (2021). In vivo confusion over in vivo conversion. Mol. Ther. *29*, 3097–3098. https://doi.org/10.1016/j.ymthe.2021.10.017.

22. Xiang, Z., Xu, L., Liu, M., Wang, Q., Li, W., Lei, W., and Chen, G. (2021). Lineage tracing of direct astrocyte-to-neuron conversion in the mouse cortex. Neural Regen. Res. *16*, 750–756. https://doi.org/10.4103/1673-5374.295925.

23. Chan, K.Y., Jang, M.J., Yoo, B.B., Greenbaum, A., Ravi, N., Wu, W.L., Sánchez-Guardado, L., Lois, C., Mazmanian, S.K., Deverman, B.E., et al. (2017). Engineered AAVs for efficient noninvasive gene delivery to the central and peripheral nervous systems. Nat. Neurosci. *20*, 1172–1179. https://doi.org/10.1038/nn.4593.

24. Lee, Y., Messing, A., Su, M., and Brenner, M. (2008). GFAP promoter elements required for region-specific and astrocyte-specific expression. Glia *56*, 481–493. https://doi.org/10.1002/glia.20622.

25. McCarty, D.M., Fu, H., Monahan, P.E., Toulson, C.E., Naik, P., and Samulski, R.J. (2003). Adeno-associated virus terminal repeat (TR) mutant generates self-complementary vectors to overcome the rate-limiting step to transduction in vivo. Gene Ther. *10*, 2112–2118. https://doi.org/10.1038/sj.gt.3302134.

26. Taschenberger, G., Tereshchenko, J., and Kügler, S. (2017). A MicroRNA124 target sequence restores astrocyte specificity of gfaABC1D-driven transgene expression in AAV-mediated gene transfer. Mol. Ther. Nucleic Acids *8*, 13–25. https://doi.org/10.1016/j.omtn.2017.03.009.

27. Srinivasan, R., Lu, T.Y., Chai, H., Xu, J., Huang, B.S., Golshani, P., Coppola, G., and Khakh, B.S. (2016). New transgenic mouse lines for selectively targeting astrocytes and studying calcium signals in astrocyte processes in situ and in vivo. Neuron *92*, 1181–1195. https://doi.org/10.1016/j.neuron.2016.11.030.

28. McBride, J.L., Boudreau, R.L., Harper, S.Q., Staber, P.D., Monteys, A.M., Martins, I., Gilmore, B.L., Burstein, H., Peluso, R.W., Polisky, B., et al. (2008). Artificial miRNAs mitigate shRNA-mediated toxicity in the brain: implications for the therapeutic development of RNAi. Proc. Natl. Acad. Sci. U S A *105*, 5868–5873. https://doi.org/10.1073/pnas.0801775105.

29. Boudreau, R.L., Spengler, R.M., and Davidson, B.L. (2011). Rational design of therapeutic siRNAs: minimizing off-targeting potential to improve the safety of RNAi therapy for Huntington's disease. Mol. Ther. *19*, 2169–2177. https://doi.org/10.1038/mt.2011.185.

30. Brulet, R., Matsuda, T., Zhang, L., Miranda, C., Giacca, M., Kaspar, B.K., Nakashima, K., and Hsieh, J. (2017). NEUROD1 Instructs neuronal conversion in non-reactive astrocytes. Stem Cell Rep. *8*, 1506–1515. https://doi.org/10.1016/j.stemcr.2017.04.013.

31. Sleat, D.E., Wiseman, J.A., El-Banna, M., Kim, K.H., Mao, Q., Price, S., Macauley, S.L., Sidman, R.L., Shen, M.M., Zhao, Q., et al. (2004). A mouse model of classical late-infantile neuronal ceroid lipofuscinosis based on targeted disruption of the CLN2 gene results in a loss of tripeptidyl-peptidase I activity and progressive neurodegeneration. J. Neurosci. *24*, 9117–9126. https://doi.org/10.1523/JNEUROSCI.2729-04.2004.

32. Chang, M., Cooper, J.D., Sleat, D.E., Cheng, S.H., Dodge, J.C., Passini, M.A., Lobel, P., and Davidson, B.L. (2008). Intraventricular enzyme replacement improves disease phenotypes in a mouse model of late infantile neuronal ceroid lipofuscinosis. Mol. Ther. *16*, 649–656. https://doi.org/10.1038/mt.2008.9.

33. Maimon, R., Chillon-Marinas, C., Snethlage, C.E., Singhal, S.M., McAlonis-Downes, M., Ling, K., Rigo, F., Bennett, C.F., Da Cruz, S., Hnasko, T.S., et al. (2021). Therapeutically viable generation of neurons with antisense oligonucleotide suppression of PTB. Nat. Neurosci. *24*, 1089–1099. https://doi.org/10.1038/s41593-021-00864-y.

Reply to *In vivo* confusion over *in vivo* conversion

We strongly disagree with Dr. Gong Chen's criticisms of our recently published *Cell* paper[1] in his recent letter to the editor.[2]

In our publication,[1] we demonstrated that stringent lineage tracing is essential for *in vivo* studies on astrocyte-to-neuron conversion. As described in Dr. Chen's prior publications,[3,4] we observed the same phenomenon: the adeno-associated virus (AAV)-expressed fluorescence reporter was detected predominantly in astrocytes in the control group and in neurons in the NEUROD1 group. On the basis of this phenomenon, Dr. Chen concluded that resident astrocytes were converted into neurons with perfect identity and connectivity by forced expression of NEUROD1. In contrast, our experiments using lineage mapping and retrograde tracing unambiguously showed that those viral reporter-labeled perfect neurons were in fact native neurons and were not derived from resident astrocytes.[1] We further showed that NEUROD1 mutants lacking neurogenic activity still induced neuronal expression of the viral reporter, ruling out the possibility of astrocyte-to-neuron conversion by forced expression of NEUROD1 in the adult mouse brain. Mechanistically, we showed that cell-type specificity of the promoter in AAVs could be altered by the downstream genes such as NEUROD1.

Regarding the issue of viral titers, Dr. Chen did not provide direct evidence that the viral reporter-labeled neurons in his publications originated from astrocytes rather than native neurons. Second, we used the same amount of virus for both the control and NEUROD1 groups; however, only the latter group showed robust leaky neuronal expression of the viral reporter, excluding a role for viral titers in such a phenomenon. This conclusion is further supported by our results following injections of a mixture of the NEUROD1 and control viruses, showing that the reporter from the NEUROD1 virus but not from the control virus was easily detected in native neurons. Third, NEUROD1-induced neuronal expression of the viral reporter was also detected in areas distant from the injection core and where the virus concentration is very low. Finally, "different groups use different methods to titer, and even for a given stock large differences can be reported, as was well illustrated in a trial where multiple groups measured the titer of the same stock, with differences of up to 100-fold reported."[5] As such, the viral titers used by Dr. Chen, us, and other groups cannot be directly compared.

Similarly, Dr. Chen's assertion that "the Cre-loxP recombination…may have created a higher barrier for cell conversion" is not supported by any available evidence. Cre-loxP-mediated lineage tracing methods have been extensively used in biological research for decades. They were also successfully applied by us and others to study cell conversions in the adult mouse brain and spinal cord.[6–13] In Dr. Chen's study using the lineage tracing method,[14] there were concerns about experimental design. As they did not use a reporter-expressing NEUROD1 virus as in all their other studies,[3,4] there was no evidence to show that those genetically labeled neurons actually were derived from NEUROD1-transduced cells. We repeated Dr. Chen's experiment by using double reporters, one for the NEUROD1 virus and the other for the lineage-traced astrocytes.[1] Despite many viral reporter-positive neurons, none showed evidence of being derived from genetically lineage-traced astrocytes.[1] Additionally, we detected occasional leakage of the genetic reporter in neurons in the mouse line that was used by Dr. Chen.[14] Such mice with neuronal leakage might explain Dr. Chen's observation of some genetically labeled neurons, but these mice should have been excluded from their study. Dr. Chen's claim of Cre toxicity in lineage tracing is self-contradictory, as his group has frequently used AAV-expressed Cre, which should be even more toxic because of higher copy numbers and expression.

Lei-Lei Wang[1] and Chun-Li Zhang[1]
[1]Department of Molecular Biology and Hamon Center for Regenerative Science and Medicine, University of Texas Southwestern Medical Center, Dallas, TX 75390, USA

https://doi.org/10.1016/j.ymthe.2022.01.027

Corresponding author
E-mail: chun-li.zhang@utsouthwestern.edu

YMTHE, Volume *30*

Supplemental Information

Limited astrocyte-to-neuron conversion in the mouse brain using NeuroD1 overexpression

David Leib, Yong Hong Chen, Alex Mas Monteys, and Beverly L. Davidson

Supplemental figure

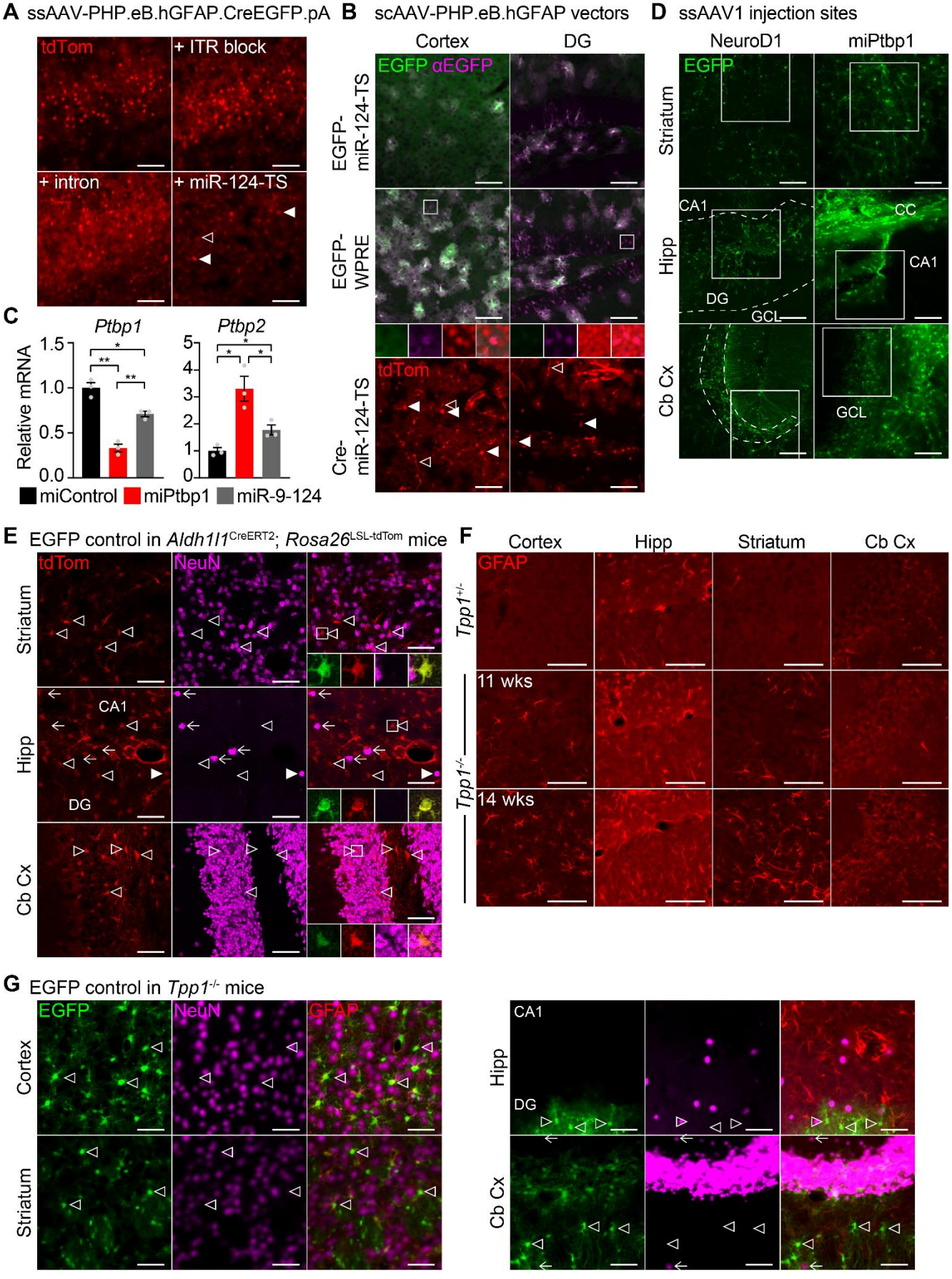

Figure S1: Supporting data

(A) tdTom fluorescence images from cerebral cortex of *Rosa26*$^{LSL\text{-}tdTom}$ mice (n=3-4) injected retro-orbitally with 1E11 vg of ssAAV-PHP-eB.hGFAP.CreEGFP.pA vectors. An inverted terminal repeat (ITR) transcription block (top right), synthetic intron (bottom left), and 3' UTR miR-124 targeting site (miR-124-TS; bottom right) were added sequentially to the original vector (top left). The ITR block had no effect, the intron increased the number of tdTom+ cells, and the miR-124-TS helped restrict tdTom expression to astrocytes, though some sparse Cre recombination still occurred in neurons (solid arrowheads) and endothelial cells (open arrowhead). No EGFP fluorescence was detected (data not shown). Scale bars, 100 µm. (B) Fluorescence images from C57BL6/J or *Rosa26*$^{LSL\text{-}tdTom}$ mice (n=2) injected retro-orbitally with scAAV-PHP-eB.hGFAP vectors. scAAV-PHP-eB.hGFAP.EGFP.miR-124-TS (3.16E11 vg; top row) transduced glia across the CNS, shown as merged EGFP direct fluorescence (green) and immunofluorescence (magenta). Replacing the miR-124-TS with a WPRE increased EGFP fluorescence despite a lower dose (1.0E11 vg; longer fluorescence exposure in top row than 2nd row). However, the WPRE vector led to low-level expression in neurons that co-stained for EGFP (magenta) and NeuN (red, insets) in the cortex and DG. scAAV-PHP-eB.hGFAP.Cre.miR-124-TS transduced glia across the CNS, but also NeuN-positive neurons (solid arrowheads) and endothelial cells (open arrowheads). Results were similar in other areas of the central nervous system, including striatum and cerebellar cortex (data not shown). Scale bars, 100 µm. (C) RT-qPCR data from Neuro-2a cells showing knockdown of *Ptbp1* and downstream upregulation of *Ptbp2* by miR-9-124 and miPtbp1 compared to miControl (n=3 biological repeats). One-way repeated-measure ANOVAs were significant for both genes (*Ptbp1*, $F=384.4$, $p=0.0008$; *Ptbp2*, $F=39.86$, $p=0.0224$), and Holm-Šídák multiple comparisons were performed (*, $p<0.05$, **, $p<0.01$). Data represent mean±SE. (D) Low-magnification confocal images showing viral EGFP expression for NeuroD1 conversion experiments (Figure 1E, 1F) and fluorescence images showing viral EGFP expression for miPtbp1 conversion experiments (Figure 1G). Regions with astrocyte-to-neuron conversion in NeuroD1-treated hippocampus and cerebellum are outlined with dashed lines. Boxed regions are included in Figures 1E and 1G. Scale bars, 100 µm. (E) Immunofluorescence from mice (n=2) injected with an EGFP control for the NeuroD1 conversion experiment in *Aldh1l1*^{CreERT2}; *Rosa26*$^{LSL\text{-}tdTom}$ mice (Figure 1E). Open arrowheads, transduced tdTom+ cells that do not co-localized with NeuN. Insets show EGFP expression (green) for a representative cell. Solid arrowhead, single tdTom+ cell that co-localized with NeuN but did not express EGFP from the AAV. Arrows, neurons with no tdTom or EGFP expression. Scale bars, 50 µm. (F) Gfap immunostaining confirming progressive astrogliosis in Tpp1$^{-/-}$ mice at 11 (n=2) and 14 weeks (n=7) of age. Images from 14-week-old mice were taken from the contralateral side of the brains in Figure 1I but displayed with brighter contrast settings. Scale bars, 100 µm. (G) Immunofluorescence from mice injected with an EGFP control (n=1) for NeuroD1 conversion in Tpp1$^{-/-}$ mice (Figure 1I). Open arrowheads, EGFP+ cells that do not co-localize with NeuN. Arrows, NeuN+ neurons that do not co-localized with EGFP. Scale bars, 50 µm. ITR, inverted terminal repeat; DG, dentate gyrus; Hipp, hippocampus; Cb cx, cerebellar cortex; GCL, granule cell layer.

Supplemental methods

Animals

Animal protocols were approved by The Children's Hospital of Philadelphia Institutional Animal Care and Use Committee. Mice were housed in a controlled temperature and humidity environment on a 12-hour light/dark cycle according to the Guide for the Care and Use of Laboratories animal. Food and water were provided ad libitum. C57BL/6J, *Aldh1l1*^{CreERT2}, and *Rosa26*$^{LSL\text{-}tdTom}$ mice were obtained from The Jackson Laboratory (JAX #000664, #031008, and #007914) and maintained in house. Tpp1$^{-/-}$ males were crossed with Tpp1$^{+/-}$ females in house to generate Tpp1$^{-/-}$ mice.

Design and *in vitro* testing of miPtbp1

An artificial microRNA targeting mouse *Ptbp1* (miPtbp1) based on a previously published shRNA (target sequence: 5'-CTCAATGTCAAGTACAACAAT-3')[1] was embedded in a microRNA backbone similar to human miR-30.[2] For *in vitro* experiments, miPtbp1 or two control microRNAs were cloned downstream of a U6 promoter. As a positive control, the combined mouse microRNAs miR-9 and -124 were used (miR-9-124), since miR-124 targets *Ptbp1*[3] and miR-9-124 has been previously shown to convert fibroblasts to neurons *in vitro*.[4] As a negative control, a previously described microRNA[5] was included.

Ptbp1 knockdown by miPtbp1 was confirmed in Neuro-2a cells. In three independent experiments, cells were seeded at 75,000 cells per well in 24-well plates and transfected with 500 ng of plasmid DNA using Lipofectamine 3000 (Invitrogen). After 48 hours, cells were rinsed once with PBS and RNA collected using Trizol (Invitrogen). cDNA was generated using MultiScribe reverse transcriptase (Invitrogen) and random priming. qPCR was then performed on a Bio-Rad CFX384 machine using TaqMan Universal Master Mix II (Applied Biosystems) and the following primer/probe mixes (ThermoFisher): *Ptbp1* (Mm01731480_gH), *Ptbp2* (Mm00497922_m1), and *Gapdh* (Mm99999915_g1). Gene expression was calculated relative to *Gapdh* and normalized to non-transfected controls within each experiment, and the combined data from multiple experiments was normalized to miSafe control. Statistical analysis was performed in Graphpad Prism 9.2.0.

Virus production

AAV shuttle plasmids were constructed with AAV2 inverted terminal repeats (ITRs) for single-stranded AAVs (ssAAVs) or modified ITRs to produce self-complementary AAVs (scAAVs),[6] the human GFAP ABC_1D promoter (hGFAP),[7] and a 6.9-kb plasmid backbone to reduce cross-packaging. Mouse *Neurod1* cDNA followed by P2A-EGFP or EGFP alone were cloned downstream of the hGFAP promoter, and miPtbp1 or miControl were cloned into the 3'UTR of EGFP. A block sequence to stop transcription from the left ITR, a synthetic intron (Addgene plasmid #99129),[8] and four tandem miR-124 targeting sequences (miR-124-TS)[9] were cloned into the specified plasmids. Plasmid sequences were confirmed by Sanger sequencing (Genewiz), and ITR integrity was confirmed by SmaI restriction digest. AAVs were produced in house by triple transfection of HEK293 cells and purification by iodixanol ultracentrifugation. The following viruses were produced:

ssAAV-PHP.eB.hGFAP.CreEGFP.SV40pA

ssAAV-PHP.eB.block.hGFAP.CreEGFP.SV40pA
ssAAV-PHP.eB.block.hGFAP.intron.CreEGFP.SV40pA
ssAAV-PHP.eB.block.hGFAP.intron.CreEGFP.miR-124-TS.SV40pA
scAAV-PHP.eB.hGFAP.intron.EGFP.miR-124-TS.SV40pA
scAAV-PHP.eB.hGFAP.intron.EGFP.WPRE.SV40pA
scAAV-PHP.eB.hGFAP.intron.Cre.miR-124-TS.SV40pA
ssAAV1.block.hGFAP.intron.NeuroD1.2A.EGFP.miR-124-TS.SV40pA
ssAAV1.block.hGFAP.intron.EGFP.miR-124-TS.SV40pA
ssAAV1.block.hGFAP.intron.EGFP.miPtbp1.SV40pA
ssAAV1.block.hGFAP.intron.EGFP.miControl.SV40pA

AAV genome titers were determined by digital droplet PCR.

Virus infusions

AAV-PHP.eB viruses were injected retro-orbitally in a volume of 100 µl. Mice were 5-10 months old for scAAV experiments in C57BL6/J and *Rosa26*$^{LSL\text{-}tdTom}$ mice (Figure 1B, 1C, S1B), and 3-4 months old for ssAAV experiments in *Rosa26*$^{LSL\text{-}tdTom}$ mice (Figure S1A).

AAV1 viruses were delivered by stereotaxic injection as previously described[10] with the following coordinates:

Cerebral cortex: +0.86 mm rostral to bregma, +1.8 mm from midline, 1.7 mm deep
Striatum: +0.86 mm rostral to bregma, 1.8 mm from midline, 3.5 mm deep
Hippocampus: 1.7 mm caudal to bregma, 1.5 mm from midline, 2.0 mm deep
Cerebellum: 1.7 mm caudal to bregma, 1.5 mm from midline, 2.0 mm deep

For NeuroD1 and miPtbp1 conversion experiments in *Aldh1l1*^{CreERT2}; *Rosa26*$^{LSL\text{-}tdTom}$ mice, mice were pre-administered tamoxifen at 75 mg/kg for five consecutive days four weeks prior to surgery. For NeuroD1 conversion experiments (Figure 1E), mice were 10-15 months old at the time of infusion. For miPtbp1 conversion experiments (Figure 1G), mice were 4-10 months old. One miPtbp1-injected mouse died following surgery. Ten-week-old Tpp1$^{-/-}$ mice were injected with ssAAV1 vectors expression NeuroD1, EGFP, miPtbp1, and miControl (n=3). At this age, Tpp1$^{-/-}$ mice are sensitive to handling, and two mice injected with EGFP, two injected with miPtbp1, and one injected with miSafe died between surgery and euthanasia.

Tissue processing, immunofluorescence, and microscopy

Mice were transcardially perfused with ice-cold PBS and 4% paraformaldehyde. Brains were post-fixed overnight and cryoprotected in 30% sucrose before sectioning at a thickness of 40 µm on a freezing microtome. For immunofluorescence, floating sections were blocked in 5% goat serum in PBS with 0.1% triton (PBS-T) at room temperature for two hours, then incubated with primary antibodies at 4ºC overnight. The following day, sections were washed four times with PBS-T, then incubated with Alexa Fluor secondary antibodies (Invitrogen) in block buffer for one hour at room temperature, washed three times, incubated with Hoechst dye (Invitrogen) for five minutes, and rinsed. Stained sections were mounted on slides and coverslipped with Fluoro-Gel (Electron Microscopy Sciences). Images were acquired on a

Leica DM6000B microscope equipped with a 10X HC PLAPO (numerical aperture (NA) 0.4) lens and a Hammatsu Orca flash 4.0 monochrome camera, or a Leica SP8 confocal microscope equipped with a 40X HC PLAPO CS2 (NA 0.75) lens and HyD photodetectors. Images were processed in ImageJ. The following primary antibodies were used: NeuN (rabbit monoclonal, dilution 1:2000, Abcam ab177487), GFAP (mouse monoclonal, dilution 1:2000, SIGMA G 3893), EGFP (chicken polyclonal, dilution 1:500, Aves GFP-1020).

Supplemental references

1. Xue, Y., Ouyang, K., Huang, J., Zhou, Y., Ouyang, H., Li, H., Wang, G., Wu, Q., Wei, C., Bi, Y., Jiang, L., et al. (2013). Direct conversion of fibroblasts to neurons by reprogramming PTB-regulated microRNA circuits. Cell *152*, 82-96. 10.1016/j.cell.2012.11.045.
2. McBride, J.L., Boudreau, R.L., Harper, S.Q., Staber, P.D., Monteys, A.M., Martins, I., Gilmore, B.L., Burstein, H., Peluso, R.W., Polisky, B., Carter, B.J., et al. (2008). Artificial miRNAs mitigate shRNA-mediated toxicity in the brain: implications for the therapeutic development of RNAi. Proc Natl Acad Sci U S A *105*, 5868-5873. 10.1073/pnas.0801775105.
3. Makeyev, E.V., Zhang, J., Carrasco, M.A., and Maniatis, T. (2007). The MicroRNA miR-124 promotes neuronal differentiation by triggering brain-specific alternative pre-mRNA splicing. Mol Cell *27*, 435-448. 10.1016/j.molcel.2007.07.015.
4. Yoo, A.S., Sun, A.X., Li, L., Shcheglovitov, A., Portmann, T., Li, Y., Lee-Messer, C., Dolmetsch, R.E., Tsien, R.W., and Crabtree, G.R. (2011). MicroRNA-mediated conversion of human fibroblasts to neurons. Nature *476*, 228-231. 10.1038/nature10323.
5. McBride, J.L., Pitzer, M.R., Boudreau, R.L., Dufour, B., Hobbs, T., Ojeda, S.R., and Davidson, B.L. (2011). Preclinical safety of RNAi-mediated HTT suppression in the rhesus macaque as a potential therapy for Huntington's disease. Mol Ther *19*, 2152-2162. 10.1038/mt.2011.219.
6. McCarty, D.M., Fu, H., Monahan, P.E., Toulson, C.E., Naik, P., and Samulski, R.J. (2003). Adeno-associated virus terminal repeat (TR) mutant generates self-complementary vectors to overcome the rate-limiting step to transduction in vivo. Gene Ther *10*, 2112-2118. 10.1038/sj.gt.3302134.
7. Lee, Y., Messing, A., Su, M., and Brenner, M. (2008). GFAP promoter elements required for region-specific and astrocyte-specific expression. Glia *56*, 481-493. 10.1002/glia.20622.
8. Chan, K.Y., Jang, M.J., Yoo, B.B., Greenbaum, A., Ravi, N., Wu, W.L., Sanchez-Guardado, L., Lois, C., Mazmanian, S.K., Deverman, B.E., and Gradinaru, V. (2017). Engineered AAVs for efficient noninvasive gene delivery to the central and peripheral nervous systems. Nat Neurosci *20*, 1172-1179. 10.1038/nn.4593.
9. Taschenberger, G., Tereshchenko, J., and Kugler, S. (2017). A MicroRNA124 Target Sequence Restores Astrocyte Specificity of gfaABC1D-Driven Transgene Expression in AAV-Mediated Gene Transfer. Mol Ther Nucleic Acids *8*, 13-25. 10.1016/j.omtn.2017.03.009.
10. Keiser, M.S., Chen, Y.H., and Davidson, B.L. (2018). Techniques for Intracranial Stereotaxic Injections of Adeno-Associated Viral Vectors in Adult Mice. Curr Protoc Mouse Biol *8*, e57. 10.1002/cpmo.57.